

PRELIMINARY RESULTS FROM A WIND TUNNEL BASED STUDY OF TAIL ROTOR BLADE VORTEX INTERACTION

F.N. Coton, R.A.McD. Galbraith
Department of Aerospace Engineering,
University of Glasgow
Glasgow, UK, G12 8QQ

Tongguang Wang
Department Of Aerodynamics
Nanjing University of Aeronautics and Astronautics
China

S. Newman
School of Engineering Sciences
University of Southampton
Southampton UK

Abstract

The paper describes a series of wind tunnel tests to simulate the interaction of a main rotor tip vortex with a tail rotor. In the experiments, which were carried out in the Argyll wind tunnel of Glasgow University, a single-bladed rotor located in the tunnel's contraction was used to generate the tip vortex which travelled downstream into the working section where it interacted with a model tail rotor. The tail rotor was instrumented with miniature pressure transducers that measured the aerodynamic response during the interaction. Preliminary results, for the given conditions, suggest that the rotor blade vortex interaction is similar in form to that previously measured on a fixed, non-rotating blade.

Nomenclature

C_p	unsteady pressure coefficient
C_{ps}	time averaged pressure coefficient
C_{p0}	initial pressure coefficient, $t=0$
c	interacting blade chord
R	tail rotor radius
r	local radius of tail rotor blade
t	sample time
V	chordwise velocity
V_∞	freestream velocity
x	chordwise distance measured from leading edge
z	vertical distance of tail rotor hub centre from wind tunnel floor
θ	blade pitch angle
Ω	tail rotor angular speed

Introduction

For many flight conditions, the tip vortices from the main rotor of a helicopter interact with the following blades and the tail rotor. This phenomenon is termed, Blade Vortex Interaction (BVI) and results in rapid (often impulsive) changes of the aerodynamic coefficients that can produce vibrations and increased radiated noise (Ref. 1). Additionally, many helicopters have encountered problems in yaw control due to the main rotor/tail rotor interaction; necessitating design changes to resolve the difficulty (Refs. 2 & 3). To date, however, most of the research has focused on the case of main rotor BVI, where the vortex interactions occur on the main rotor disk. Of particular note are the studies carried out by Strauss et al. (Ref. 4) and Masson et al. (Ref. 5) among many others. Unfortunately far less work has been performed for the nominally orthogonal interaction; typical of a main rotor vortex interacting with a tail rotor blade.

In forward flight, the tip vortex from a helicopter main rotor blade may be ingested into the tail rotor disc and severed by the tail-rotor blades. These interactions occur at various angles, with the limiting case of orthogonality. Both theoretical and computational investigations of the orthogonal blade vortex interactions (Refs. 6-10) have concluded, that the vortical interaction is significantly influenced by the axial flow within the vortex core. If the axial flow is directed toward the cutting surface, the core bulges and, if the axial flow is away from the surface, the core thins (see Fig. 1). This kind of vortex core distortion has been verified by flow visualisation (Refs. 9-11), and the interaction of the core flow with the cutting blade generally results in significant pressure differences between the blade surfaces (Refs. 12 & 13). The studies also showed the

production of secondary vorticity and entrainment of the blade boundary layer into the core, indicating the complexity of the orthogonal BVI.

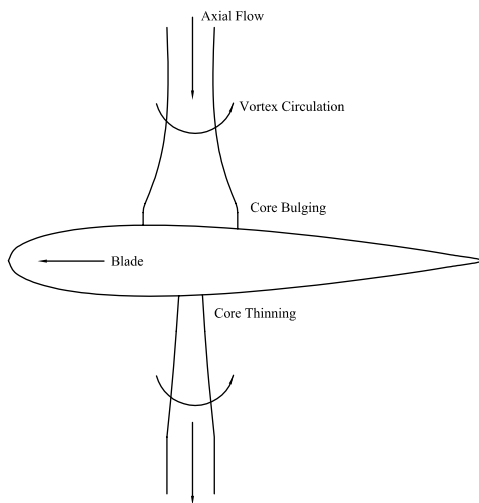


Fig. 1. Illustration of orthogonal blade vortex interaction

More recently, a series of experimental investigations of orthogonal BVI were conducted at the Glasgow University 1.15 m x 0.85 m low speed wind tunnel (Refs. 14-19). A novel vortex generator was used, which consisted of a one-bladed rotor rig, with the rotational axis located in the tunnel's contraction. As the rotor rotated, the blade was pitched to generate a transverse vortex that was convected through the wind tunnel and subsequently cut by a test blade in the working section. The experiment gave good results of orthogonal BVI from which it was identified that, as the vortex collided with the leading edge of the test blade, it experienced a strong suction peak and a pressure pulse on opposite surfaces. The orthogonal BVI study was then continued in the Glasgow University larger 2.65 m x 2.04 m low speed wind tunnel (Ref. 20). In the latter experiment, the new vortex generator produced more stable vortices with very little "wander". These vortices provided good temporal resolution for different interacting blade settings.

However, as far as the authors are aware, all orthogonal BVI wind tunnel test studies have so far focused on the interaction with a stationary blade, although the effect of multiple vortex cuttings, which may occur within the tail rotor plane, has been examined by placing a blade upstream of another instrumented blade (Ref. 15). Understandably, due to the flow and modelling complexities, only in hover and in

climbing flight has the rotating tail rotor interaction with a main rotor been simulated numerically (Ref. 21); where the orthogonal vortex cutting is unlikely. Ellin (Ref. 22) reported a flight trial carried out to collect data on tail rotor aerodynamic performance under influence of the main rotor wake. His results showed that the main rotor tip vortex could interact with the tail rotor blade in low speed forward flight producing changes in local chordwise velocity and incidence at the blade with consequent variations in blade loading. The flight tests of Leverton et al., (Ref. 23) considered the subjectively distinctive noise generated by the interaction of the tail rotor with the main rotor tip vortex. Given, however, the scarcity of information available, wind tunnel pressure measurements on a rotating tail rotor in the presence of a main rotor potentially provide very valuable insight into the phenomenon.

Whilst the interactions with a fixed blade are very informative, they may not be appropriately modelling the actual interaction. This can be appreciated by considering that, as the main rotor tip vortex approaches the tail rotor, in helicopter forward flight, the tail rotor flowfield affects the vortex and adds an additional induced velocity from the tail rotor vortex system to the main vortical flow. Thus, the interaction with a rotating blade may differ from that with a stationary blade. If it does, interest then centres on the extent to which the two cases differ. In particular, if the ratio of the freestream velocity is high with respect to the rotational velocity of the main rotor, there is likely to be little deformation of the vortex prior to vortex cutting. This would suggest similarity of the important and initial phases of the interaction, where the main impulsive response is manifest, with only the latter stages of the interaction being different. To gain insight into this, a preliminary experiment was conducted in the 2.65m x 2.04m wind tunnel in June, 2001 in which a two bladed instrumented rotor was installed in the tunnel's working section (Fig. 2). In the pressure data collected there was clear evidence of the interactions that, from preliminary considerations, exhibited the telltale signs of suction and compression on either side of the rotor blade.

Experimental Design

By consideration of the geometry of the tail rotor interaction problem, it is possible to establish which sectors of the disk are likely to experience primary interactions and which sections of the disk could experience interaction with an already pre-cut vortex. This

depends on the advance ratio of the rotor which, in this case, effectively represents the relationship between the rate of downstream passage of the vortex and the speed of rotation of the rotor blades.

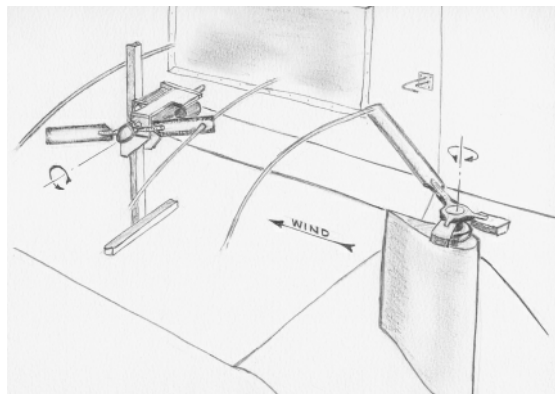


Fig. 2. Illustration of test set-up

Figure 3 presents a plot showing the minimum tail rotor Advance Ratio required to achieve single vortex interactions on a two-bladed tail rotor at three radial positions corresponding approximately to the measurement locations used during the test programme, i.e. $r/R = 0.7$, 0.75 and 0.8 . The assumed direction of rotation of the tail rotor is also the same as that used in the experiment. The results presented in the figure assume that the vortex convects in a horizontal line at constant velocity across the tail rotor at a series of defined distances from the rotor axis. Thus, if the azimuth at which a blade initially interacts with the vortex is then chosen, the potential for multiple cutting depends on whether the vortex passes over the rotor disk before the following blade makes contact with it. It may be observed from the figure that single interactions are possible at any location on the upper half of the tail rotor, where the blades move in the same direction as the free stream, provided the Advance Ratio is above 0.3. The same is not true on the lower half of the disk where the blades move into the onset flow. In this case, it is almost impossible to sustain single interactions on the disk if the initial interaction occurs near the front of the disk.

On the basis of the above, it is clear that the potential for single interactions can be maximised if the Advance Ratio is kept above 0.3 during tests. For this reason, the main body of the test programme was conducted at an Advance Ratio of approximately 0.42.

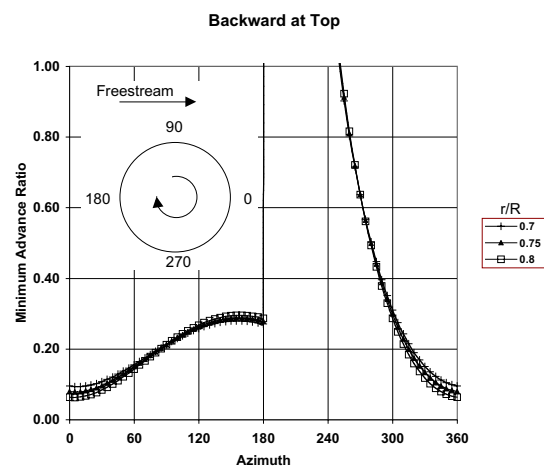


Fig. 3 Minimum Advance Ratios required to achieve single vortex interactions at three radial locations.

Experimental Methods

The experiments were conducted in the Glasgow University 2.65 m x 2.04 m Argyll low speed wind tunnel. This is a closed return facility with a maximum operating speed of 76 m/s. During testing, the freestream velocity and temperature were monitored continuously.

A vortex generator consisting of a NACA 0015 cross-section, single-bladed rotor of radius 0.16m and chord 0.16m was placed in the contraction of the wind tunnel. The rotor hub was fully articulated and incorporated flap and lag hinges with a cantilevered flap spring and elastomeric lag dampers. The rotor was rotated by a variable-frequency drive motor. During rotation, the blade pitch was varied using a spring loaded pitch link running on a cylindrical cam configured such that the blade pitch varied smoothly in four equivalent (90°) phases of azimuth. The first phase set the blade at zero incidence while the blade was pointing into the settling chamber (45° azimuthal travel on either side of the wind tunnel centre line). In the next two phases of motion, the blade was pitched from zero to 10° , before traversing the working section at a constant 10° incidence. In the final 90° phase, the spring-loaded pitch link forced the blade to overcome its aerodynamic and inertial loads and follow the cam as it returned to zero degrees. In this way, a series of vortices were created in the wind tunnel separated in time by one rotor revolution. These curved, three-dimensional vortices were then convected through the wind tunnel working section.

Prior to conducting interaction experiments, velocity measurements of the convecting

vortex were made using a TSI IFA-300 constant temperature hot wire Anemometer system using DANTEC P61 cross wire probes. The probes used $5\ \mu\text{m}$ diameter plated tungsten wires with a length-to-diameter ratio of 250. The measuring volume of each probe was approximately 0.8 mm in diameter and 0.5 mm in height.

For the blade-vortex interaction experiments, a tail rotor was placed in the path of the convecting vortex in order to study the vortex interaction with a rotating blade (Fig. 2). The tail rotor system, which had been designed at the University of Southampton, was supplied by Westland Helicopters Limited, but the blades were re-designed and constructed by the University of Glasgow in order to accommodate appropriate pressure transducers. The rotor had two constant-chord blades of the NACA0015 aerofoil section. The radius of the rotor was 428 mm and the chord of the blades was 100mm. One of the blades was instrumented with nine miniature Sensym pressure transducers mounted on the upper surface and six on the lower surface (Fig. 4). The transducers were arranged in three chordal arrays, the distances of which from the rotational centre were 69%, 75% and 81% of the rotor radius. Each chordal array had three transducers on the upper surface, positioned at 6%, 30% and 75% of the chord, and two on the lower surface, located at 10% and 65% of the chord.

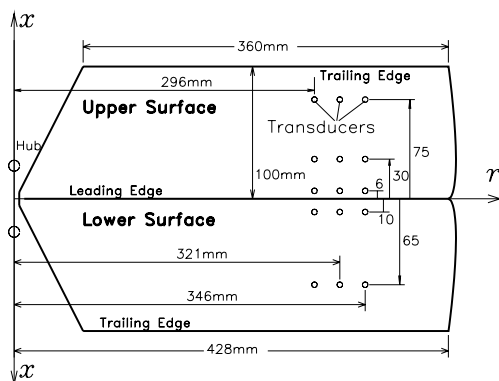


Fig. 4. Pressure transducer layout

The rotor was driven by a DC motor through a belt and pulley system. The rotor head was connected to two concentric shafts which were supported on two bearings mounted in a aluminium frame. The outer shaft was used to transmit the required torque to the rotor head and the inner provided changes to the blade pitch via a stepper motor connected to a ballscrew. The ballscrew nut displacement,

fore and aft, provided a relative displacement of the inner shaft with respect to the outer shaft. This relative displacement in turn, through the spider-head and pitch links, produced the desired pitch angle on the blades.

The experimental set-up allowed the tail rotor to be mounted in three different vertical positions in order to examine different vortex cutting geometries. The corresponding heights of the rotor hub centre from the wind tunnel floor are listed in Table 1. The tail rotor was installed such that the axial core flow of the vortex was toward the rotor disc from the "clean" side (Fig. 2), thus keeping the disturbance of the rotor driving and support systems on the vortex minimal prior to the vortex collision. The rotor centre was about 4 m downstream of the vortex generator rotor axis. In order to avoid the turbulent wake of the vortex generator support shaft the tail rotor was placed such that the rotational plane was on the right side 370 mm from the tunnel centre-line, facing into the settling chamber (Fig. 5). At this position, the vortex had been predicted to collide nominally orthogonally with the blade using a free-wake method coupled to a panel method simulation of the wind tunnel wall constraint (Ref. 24).

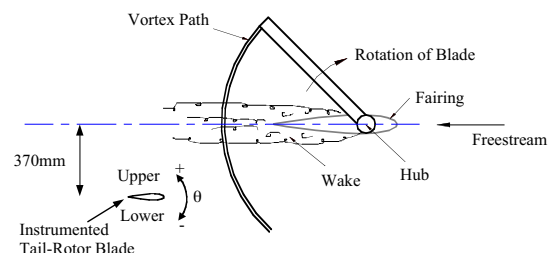


Fig. 5. Plan view of wind tunnel set-up showing lateral position of tail rotor

The direction of the rotation of the tail rotor, in all experiments, was top blade backwards with respect to the free stream flow.

Test Programme

The test programme consisted of measuring the unsteady pressures during vortex cutting by the tail rotor blade. To guarantee a severance of the vortex by the rotating blade, it was essential to know the vortex passage height at the rotor position. This height varied with the free stream speed and the rotational speed of the vortex generator. Vortex passage heights for the same vortex generator had been determined in a previous study of vortex interaction with a stationary blade (Ref. 20). It

was, however, found that the vortex height was significantly changed in this study possibly due to the larger blockage of the tail rotor system. For this reason, a hot-wire probe was mounted close to and in parallel with the tail rotor. This probe was used to detect the vortex core passage height and to monitor the vortex passage during the tests.

In the test programme reported here, tests were conducted at free stream velocities of 16 m/s and 30 m/s and three different tail rotor hub heights were used; $z = 920\text{mm}$, 760mm and 600mm measured from the wind tunnel floor. In all cases, the rotational speed of the vortex generator was fixed at 400 revolutions per minute (RPM).

In order to examine the effect of tail rotor inflow on the interaction, the thrust on the rotor was varied by changing the pitch angle, θ , of the tail rotor blades from 0° to 12° . The increased loading resulting from the blade pitch limited the rotational speed of the tail rotor to 1600 RPM for $\theta \leq 6^\circ$ and at 800 RPM for $\theta \geq 8^\circ$.

In each case, pressure data were acquired in 16 blocks of 2000 samples each. The sampling rate was 13330Hz for the rotational speed of 1600 RPM and 6670Hz for the 800 RPM cases. In this way, each block of 2000 samples contained data from four revolutions of the tail rotor. The vortex generator and the tail rotor were not synchronised and so it was possible for the instrumented blade to miss the vortex as it passed through the swept area of the rotor. For this reason a triggering pulse was supplied to the data acquisition system when the vortex generator was in a specific position. This ensured that the 16-blocks of data contained at least one vortex interaction.

Results

Vortex Parameters

The characteristics of the vortex wake produced by the vortex generator have been measured and reported in a previous study (Ref. 20). For the purposes of the present study, it is important to note that, in addition to its rotational component, the tip vortex also exhibited an axial core flow of around 2m/s.

It had been found that, for rotational speeds less than 300RPM, the vortex generator produced a series of equi-spaced well defined tip vortices. Above this speed, the generator wake contained a secondary vortex structure between each tip vortex. In fact, at rotational

speeds around 400rpm the secondary vortex became stronger than the tip vortex. This is illustrated in Fig. 6 where the measured vertical velocity component for a generator speed of 420rpm and a free stream velocity of 50m/s is presented. In this figure the strength of the secondary, counter-rotating vortex is significantly greater than the primary vortex that the generator was designed to produce. It is possible that the counter-rotating vortex may be attributed to the flapping motion of the blade. Only, however, through a dynamic study of the rotor/hub combination could an understanding of this event be known. However, the very periodic nature of the disturbance may suggest that its origin exists at the blade tip. The two vortices are, however, separated by a time period of about 0.07 seconds which, even at the lowest free stream velocity used in this study would result in a distance between the tip and secondary vortices of around 1.1m. which is more than one tail rotor diameter. By azimuth locking the triggering of data collection, it was possible to determine which of the two vortices were interacting with the tail rotor at a given time. The counter-rotating vortex, therefore, had little influence on the collected data.

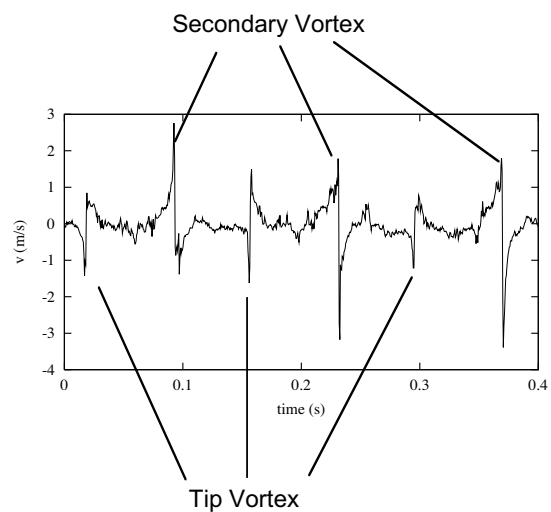


Fig. 6. Vertical velocity measurement during passage of vortex for a vortex generator speed of 420rpm.

Previous Measurements of Vortex Interaction With a Stationary Blade

Doolan et al. (Refs. 14, 17 & 20) described the unsteady surface pressure variations experienced by a blade set at zero incidence during orthogonal blade vortex interaction. Figures 7 illustrate typical temporal variations of the upper and lower surface pressure distributions due to the passage of the vortex

core over the chord. The lower surface of the blade is defined as the cutting surface toward which the axial flow is directed and the upper surface as the side from which the axial flow is away. The directions of positive and negative blade incidence are also defined on this basis. In Figs. 7, the initial value of the pressure at time $t = 0$ (C_{p0}) has been removed from the unsteady data (C_p) for clarity. To increase the clarity of the plots further, only every sixteenth data sample is presented. If the vortex deformation is negligible prior to interaction, the pressure distribution C_{p0} at the sample time $t = 0$ can be regarded as the clean pressure on the blade surface in a flow field with vortex induction. Therefore, the value of $-(C_p - C_{p0})$ on the vertical axis represents the net contribution of the interaction to the surface pressure. The other two axes in the plot denote the chordal position (x/c) and the non-dimensional time (Vt/c), respectively.

At $z/c=0$, the upper surface data in Fig. 7a shows a strong suction peak at the leading edge when the vortex encounters the blade. The subsequent passage of the vortex over the surface produces a suction ridge that abates towards the trailing edge. Meanwhile, the interaction retains its influence on the upper surface loading in the form of increased suction in the leading edge region. In fact, the vortex has passed downstream by several chord lengths before the pressure returns to its clean value C_{p0} .

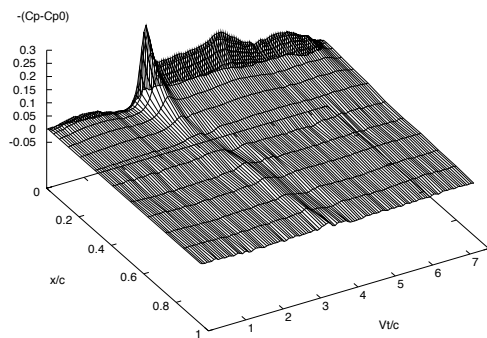


Fig. 7a Upper surface pressure response during the interaction of the vortex with a stationary blade

For the lower surface, Fig. 7b, an increase in pressure occurs just downstream of the leading edge when the vortex collides with the blade. With the passage of the vortex over the chord, this impacting pressure decreases and eventually the pressure ridge transforms into a slight suction ridge. The magnitude of the pressure and suction ridges on the lower surface is less than that of the suction ridge on the upper surface.

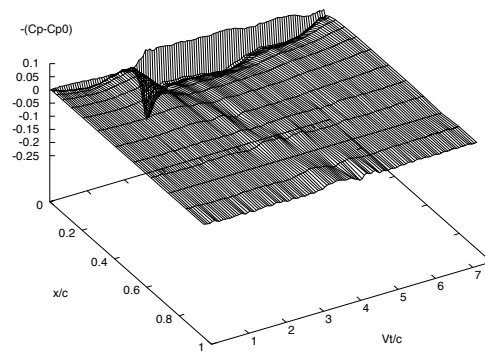


Fig. 7b Lower surface pressure response during the interaction of the vortex with a stationary blade

As the distance between the measurement station and the vortex core is increased, in the spanwise direction, the effects described above gradually diminish in magnitude with some interesting differences between measurement positions on either side of the core. The basic form of the interaction is, however, similar.

Measurements of Tail Rotor Interaction

In this section, results are presented for the case of the model tail rotor interacting with the tip vortex from the vortex generator. Since there were only five pressure transducers in each chordal array, it is not possible to present surface pressure distributions of the type shown in Figs 7. Instead, the pressure time histories for individual transducers are presented and compared for cases with and without an interacting vortex. Once again, in all of the results presented in this section, the upper surface has been defined as the side toward which the vortex axial flow is directed.

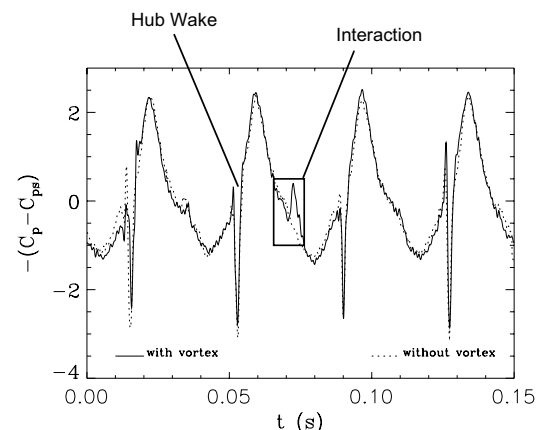


Fig. 8. Pressure coefficient variation near upper surface leading edge of tail rotor ($x/c = 0.06$, $r/R = 0.81$, $V_\infty = 30$ m/s and $\theta = 0^\circ$, $\Omega = 1600$ rpm)

An example of the data collected for one of the transducers closest to the leading edge on the upper surface ($x/c = 0.06$, $r/R = 0.81$) is shown in Fig. 8. This figure shows two overlaid measured pressure coefficient variations for four rotations of the tail rotor for wind speed $V_\infty = 30$ m/s and a blade pitch angle of $\theta = 0^\circ$. One set of data was measured with the vortex generator switched off (dotted line) and the other with it running normally (full line). The figure contains features that are common to all of the results presented in this section and is annotated to aid interpretation.

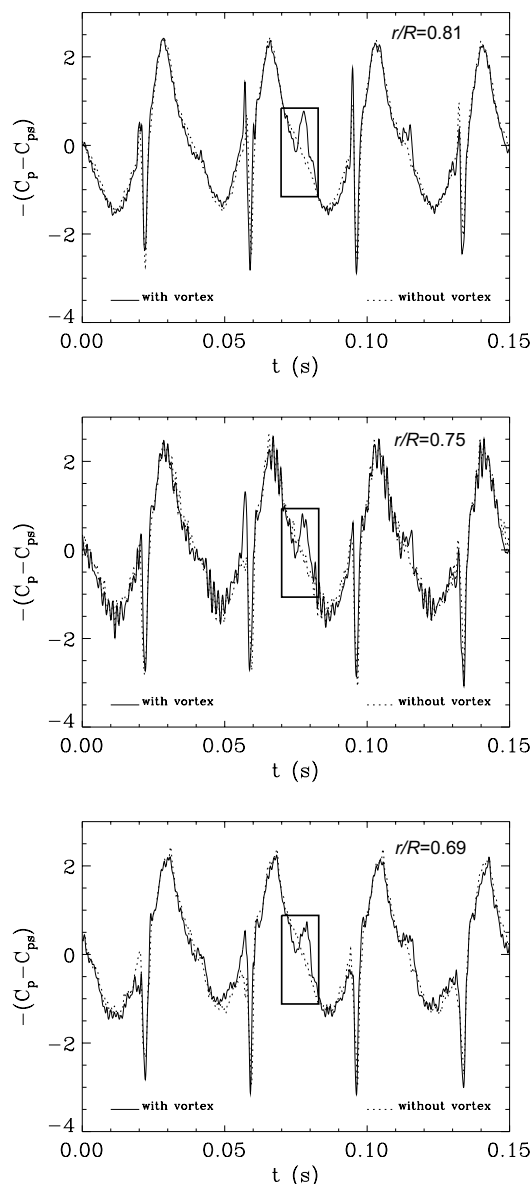


Fig. 9. Pressure coefficient variation near upper surface leading edge of tail rotor ($x/c = 0.06$, $V_\infty = 30$ m/s and $\theta = 2^\circ$, $\Omega = 1600$ rpm) at three span positions ($r/R = 0.81, 0.75$ & 0.69)

One of the main features of Fig. 8 is the cyclic variation in the level of the pressure coefficient.

The relative motion of the tail rotor blade with respect to the free stream velocity causes this. When the tail rotor is below the rotor axis and moving into the oncoming wind the dynamic pressure on the blade is greater than when it is moving above the rotor axis in the same direction as the wind. Another significant feature of the plot is the sharp downward spike in each cycle. This corresponds to the passage of the rotor blade through the wake of the hub and is accompanied by severe, high frequency, blade flapping. The severity of this is primarily due to the physical scaling of the tail rotor dimensions and its effect on the hub wake. The tail rotor interaction in this figure occurs when the blade is just above centre on the front of the tail rotor disk and is framed by a rectangular box. The interaction is characterised by a sharp increase in the leading edge suction in a similar manner to that observed during measurements on the stationary blade.

The way in which the interaction manifests itself on the rotor blade is now examined in more detail for a case in which the wind speed was set at 30m/s and the blade pitch angle to 2° . Figure 9 shows the pressure coefficient variation on the upper surface $x/c=0.06$ at three different radial positions. In each case, there is evidence of blade vortex interaction in the same sector of the cycle. The severity of the interaction appears to be almost identical at each span position. The vortex core diameter in these tests has been estimated to be around 180mm. This compares to the spacing between the innermost and outermost measurement position in Fig. 9 which is only 51mm. Previous studies (Refs. 14, 17 & 20) on a stationary blade suggest that, if the core of the vortex was aligned with any of the measurement arrays in this case the difference between the response at that array and the other arrays would be minimal.

Figure 10 shows the response at the corresponding leading-edge transducers on the lower surface. The previous studies on the stationary blade would suggest that the response should be quite different on this side of the blade. In fact, it would be anticipated that, rather than increased suction, the lower surface leading edge would experience a rise in pressure during the interaction due to the axial core flow impinging on the surface. This is indeed the case at all three of the pressure transducers showing an increase in pressure during the interaction. In a similar manner to the upper surface response, there is little difference between the response at the three spanwise positions.

The manner in which the interaction develops over the chord has been studied at great length in the previous phase of the work on the stationary blade. It has been noted that, on the upper surface, the sharp rise in leading edge suction created during the initial impact of the vortex is relatively short lived and very much confined to the leading edge region. Further down the chord there is still an increase in suction during the passage of the vortex but it is much smaller and often imperceptible depending on the proximity of the measurement station to the vortex core location (Ref. 20).

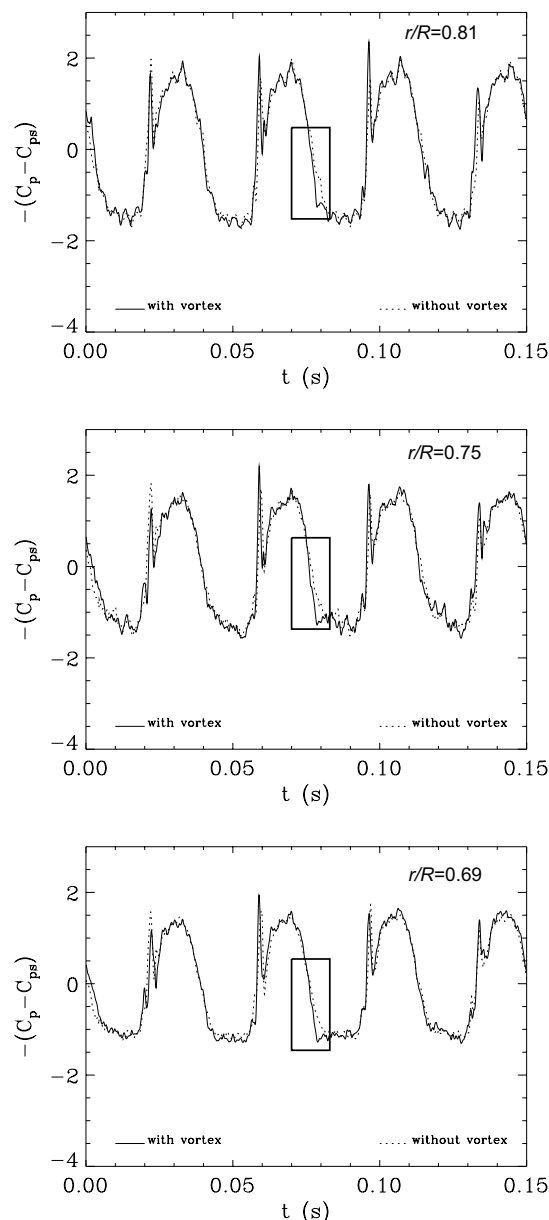


Fig. 10. Pressure coefficient variation near lower surface leading edge of tail rotor ($x/c = 0.10$, $V_\infty = 30$ m/s and $\theta = 2^\circ$, $\Omega = 1600$ rpm) at three span positions ($r/R = 0.81, 0.75$ & 0.69)

Figure 11 shows pressure coefficient variations measured at two locations on the upper surface of the rotor blade for the same test case as that presented in Figs 9 and 10. The specific locations are both at radial position $r/R=0.69$ but lie further down the chord. In fact, comparison of the two plots in this figure with the last plot in Fig. 9 allows the pressure response due to the chordal progression of the vortex to be observed. It is immediately obvious that, by the time the vortex has progressed to 30% of chord, the additional suction due to the vortex cutting has diminished substantially. Indeed, at this location only a very small disturbance, in terms of both duration and magnitude, can be detected.

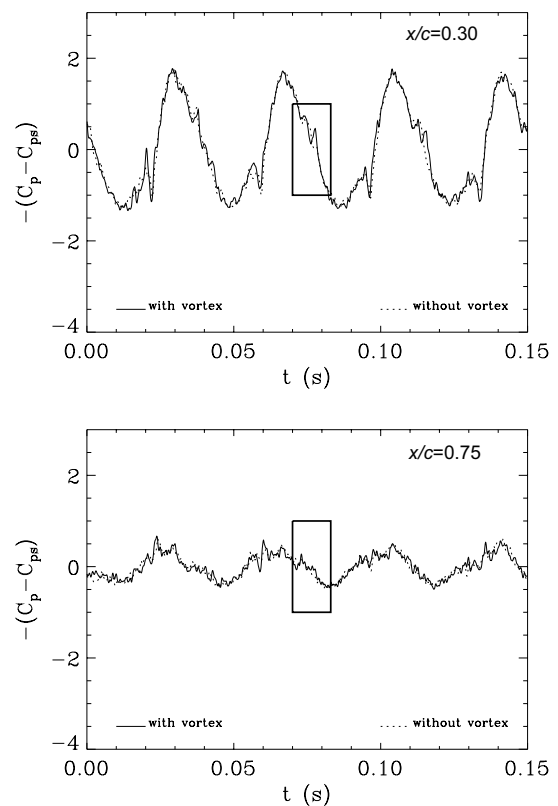


Fig. 11. Pressure coefficient variation at two upper surface locations on the tail rotor blade ($x/c = 0.30$ and 0.75 ($V_\infty = 30$ m/s and $\theta = 2^\circ$, $\Omega = 1600$ rpm, $r/R = 0.69$))

Further down the chord at $x/c = 0.75$ there is no obvious sign of any change in the level of the pressure coefficient compared with the 'no vortex' case. Taken with the other results at this radial position, this suggests that the gross behaviour is indeed similar to that previously measured on the stationary blade.

Conclusions

Tests have been conducted in a wind tunnel to simulate the interaction of a main rotor tip vortex with a tail rotor. The unsteady pressure response on the tail rotor blades during interaction has been measured using miniature pressure transducers. It has been found that the response is characterised by increased suction and pressure on opposite sides of the blade leading edge. This is, however, short-lived and does not persist as the vortex travels over the chord. The general features of this response are similar to that previously measured on a non-rotating blade during vortex interaction.

Acknowledgements

This work was funded by the Engineering and Physical Sciences Research Council, the Defence Evaluation and Research Agency, Farnborough and GKN-Westland Helicopters Ltd under grant number GR/L 58231. The authors would also like to thank the technical staff of the Department of Aerospace Engineering at Glasgow University for their valuable assistance.

References

- ¹ Sheridan, P. F. and Smith, R. P., "Interactional aerodynamics - a new challenge to helicopter technology," *J. American Helicopter Society*, Vol. 25, No. 1, 1980, pp. 3-21.
- ² Prouty, R. W. and Amer, K. B., "The YAH-64 empannage and tail rotor - a technical history," *Proc. 38th American Helicopter Society Annual National Forum*, 1982, pp. 247-261.
- ³ Brocklehurst, A., "A significant improvement to the low speed yaw control of the Sea King using a tail boom strake," *11th European Rotorcraft Forum*, 1985.
- ⁴ Straus, J., Renzoni, P., and Mayle, R., "Airfoil pressure measurements during a blade-vortex interaction and comparison with theory," *AIAA J.*, Vol. 28, 1990, pp. 222-228.
- ⁵ Masson, C. A., Green, R. B., Galbraith, R. A. M., and Coton, F. N., "Experimental investigation of a loaded rotor blade's interaction with a single vortex," *Aeronaut. J.*, Vol. 102, No. 1018, 1998, pp. 451-457.
- ⁶ Marshall, J. S., "Vortex cutting by a blade, part 1: general theory and a simple solution," *AIAA J.*, Vol. 32, No. 6, 1994, pp. 1145-1150.
- ⁷ Marshall, J. S. and Yalamanchili, R., "Vortex cutting by a blade, part 2: computations of vortex response," *AIAA J.*, Vol. 32, No. 7, pp. 1428-1436.
- ⁸ Marshall, J. S. and Grant, J. R., "Penetration of a blade into a vortex core: vorticity response and unsteady blade forces," *J. Fluid Mech.*, Vol. 306, 1996, pp. 83-109.
- ⁹ Marshall, J. S. and Krishnamoorthy, S., "On the instantaneous cutting of a columnar vortex with non-zero axial flow," *J. Fluid Mech.*, Vol. 531, 1997, pp. 41-74.
- ¹⁰ Lee, J. A., Burggraf, O. R., and Conlisk, A. T., "On the impulsive blocking of a vortex jet," *J. Fluid Mech.*, Vol. 369, 1998, pp. 301-331.
- ¹¹ Krishnamoorthy, S. and Marshall, J. S., "Three-dimensional blade vortex interaction in the strong vortex regime," *Physics of Fluids*, Vol. 10, No. 11, 1998, pp. 2828-2845.
- ¹² Ahmadi, A., "An experimental investigation of blade-vortex interaction at normal incidence," *AIAA J.*, Vol. 23, No. 1, 1986, pp. 47-55.
- ¹³ Johnston, R. T and Sullivan, J. P., "Unsteady wing surface pressures in the wake of propeller," *AIAA Paper 92-0277*, 1992.
- ¹⁴ Doolan, C. J., Coton, F. N., and Galbraith, R. A. M., "Surface pressure measurements of the orthogonal vortex interaction," *AIAA J.*, Vol. 39, No. 1, 2001, pp. 88-95.
- ¹⁵ Doolan, C. J., Coton, F. N., and Galbraith, R. A. M., "The effect of a preceding blade on the orthogonal vortex interaction," *56th American Helicopter Society Forum*, Virginia Beach, May 2000.
- ¹⁶ Doolan, C. J., Green, R. B., Coton, F. N., and Galbraith, R. A. M., "The orthogonal blade-vortex interaction experimental programme at the University of Glasgow," *26th European Rotorcraft Forum*, The Hague, Sept. 2000.
- ¹⁷ Doolan, C. J., Coton, F. N., and Galbraith, R. A. M., "Three-dimensional vortex interactions with a stationary blade," *Aeronaut. J.*, Vol. 103, No. 1030-1099, pp. 579-587.
- ¹⁸ Doolan, C. J., Coton, F. N., and Galbraith, R. A. M., "Measurements of three-dimensional vortices using a hot-wire anemometer," *AIAA Paper 99-3810*, 1999.
- ¹⁹ Green, R. B., Doolan, C. J., and Cannon, R. M., "Measurements of the orthogonal blade-vortex interaction using a particle image velocimetry technique," *Exp. Fluids*, Vol. 29, 2000, pp. 369-379.
- ²⁰ Wang, T., Doolan, C. J., Coton, F. N., and Galbraith, R. A. M., "An experimental study of the three-dimensionality of orthogonal blade-vortex interaction," *To be published AIAA Journal*, 2002.
- ²¹ Yin, J. P. and Ahmed, S. R., "Helicopter main-rotor/tail-rotor interaction," *J. American Helicopter Soc.*, Vol. 45, No. 4, 2000, pp. 293-302.
- ²² Ellin, A. D. S., "Lynx main rotor/tail rotor interactions: mechanisms and modelling,"

Proc. I. Mech.E. Part G: J. of Aerospace Eng.,
Vol. 208, No. 2, 1994, pp. 115-118.

²³Leverton, J. W., Pollard, J. S., and Wills, C.
R., "Main rotor wake/tail rotor interaction,"
Vertica, Vol. 1, 1977, pp. 213-221.

²⁴Copland, C. M., *The generation of transverse
and longitudinal vortices in low speed wind
tunnels*, PhD thesis, Univ. of Glasgow, 1997